

## Selective catalytic reduction of NO on copper-exchanged zeolites: the role of the structure of the zeolite in the nature of copper-active sites

C. Torre-Abreu<sup>a</sup>, C. Henriques<sup>a</sup>, F.R. Ribeiro<sup>a</sup>, G. Delahay<sup>b</sup>, M.F. Ribeiro<sup>a,\*</sup>

<sup>a</sup> Instituto Superior Técnico, Dep. Eng. Química, Av. Rovisco Pais, 1049-001 Lisbon Codex, Portugal

<sup>b</sup> Laboratoire de Matériaux Catalytiques et Catalyse en Chimie Organique, UMR 5618 CNRS, ENSCM, 8 Rue de l'Ecole Normale, 34053 Montpellier Cedex, France

### Abstract

Copper-exchanged zeolites with different structures (CuMFI, CuMOR and CuY) used as catalysts on the selective catalytic reduction (SCR) of NO by propene have been studied. Different types of Cu species were identified ( $\text{Cu}^{2+}$ ,  $\text{Cu}^+$ , and  $\text{CuO}$ ) by  $\text{H}_2$ -TPR and NO TPD. The structure of each zeolite determines the nature and concentration of those species and the catalytic behavior for SCR of NO by propene in the presence of oxygen. A correlation was observed between the catalytic activity, and the presence of isolated  $\text{Cu}^{2+}$  species, which is enhanced by MFI structure. ©1999 Elsevier Science B.V. All rights reserved.

**Keywords:** Copper-exchanged zeolite; CuMFI; CuMOR; CuY; NO; Selective catalytic reduction (SCR); NO TPD;  $\text{H}_2$ -TPR

### 1. Introduction

Copper-exchanged zeolites have been widely studied in their structural aspects and catalytic activity for NO decomposition and selective catalytic reduction (SCR) by hydrocarbons [1,2]. MFI zeolites appear to be the most favorable and have been the object of intense research [3,4]. Several aspects concerning the structure and function of Cu-MFI catalysts have begun to be clarified, and some consensus has been emerging, mainly in the case of NO decomposition. The NO decomposition is a redox process, involving two copper atoms in close proximity and the active species are monovalent copper ions [5].

On the SCR process much knowledge has been gained, but due to the complexity of the reactant system and divergences in the proposed mechanisms [4,6]

(redox mechanism; oxidation of NO to  $\text{NO}_2$  that reacts with hydrocarbons; oxidative reaction of hydrocarbons with NO forming an intermediate by reaction with  $\text{NO}_x$ ) many aspects of the catalysts behavior remain to be discussed and elucidated. In particular, the relation between the copper redox chemistry, the dispersion and location of copper in zeolite and the reaction mechanism have merited special attention.

Many authors agree that copper is necessary to activate NO or to form  $\text{NO}_2$ , with Cu(I) and Cu(II) species being involved [7–10] and others [11,12], assuming the redox mechanism, suggest that the maintenance of a proper balance between Cu(I) and Cu(II) is essential for good catalytic activity. The main divergence centers around the identification of the active copper species.

The majority of the Cu will be present as  $\text{Cu}^{2+}$  under the strongly oxidizing conditions, which characterize the lean  $\text{NO}_x$  operating regime. However, some authors identified the presence of  $\text{Cu}^+$  species within the

\* Corresponding author. Fax: +351-1-8417246  
E-mail address: qfilipa@alfa.ist.utl.pt (M.F. Ribeiro)

zeolite under those conditions, and proposed that NO decomposition reaction occurs over  $\text{Cu}^+$  sites [11,13] and that the hydrocarbon reductant is responsible for maintaining a reasonable concentration of active  $\text{Cu}^+$  sites during the course of the reaction. Shelef et al. [9] proposed that the active sites for the lean  $\text{NO}_x$  reaction are isolated, irreducible,  $\text{Cu}^{2+}$  ions, and Petunchi [7,8] reported that it is important to have oxidizing conditions in order to prevent the reduction of  $\text{Cu}^{2+}$  to lower oxidation states. Sachtler et al. [14] indicated that the formation of adsorbed  $\text{NO}_2$  on  $\text{Cu}^{2+}$  sites is the determining step of the reaction.

The type of metallic species that have been identified in zeolites, their coordination and electronic configuration, are influenced by the structure and composition of the zeolite, and by the specific nature and content of the metal [15–21].

The effect of the zeolite structure can be associated with the geometrical positions in which the exchanged metal is implanted, or with the microporosity of the zeolite as was suggested by Yokoyama et al. [15] for MFI structure and by Li et al. [16] for FER. Iwamoto et al. [1,17,18] found that Cu ions implanted in MFI structures exhibit higher activity than in other zeolites, e.g. in Y, mordenite and ferrierite. Wichterlovà et al. [19,20] have shown the differences in the structure of copper sites active for the decomposition and SCR of NO, correlated to the Cu sitting and redox properties of Cu ions which depend on the geometry of the zeolite matrix and Cu/Al and Si/Al compositional ratios. Based on adsorption results, Parrillo et al. [21] showed that the catalytic properties of Cu-Y and Cu-MFI are very different, even when samples having similar Si/Al ratios and Cu contents are compared. These differences are attributed to the instability and aptitude for migration of the exchanged Cu in Y zeolites, due to the more open structure of Y zeolites and the lack of five-membered-ring pockets, which are present in ZSM-5.

In this work our main goal has been to identify the principal copper species present in several as-prepared samples of zeolites with different structures (MFI, MOR and Y zeolites) and establish a correlation between the copper species and their catalytic importance for NO SCR with propene. For this study, we used zeolite samples with similar compositions and Cu/Al ratios in a wide range of Si/Al ratios and Cu exchange levels.

## 2. Experimental

### 2.1. Catalyst preparation

The parent MFI and Y zeolites in the protonic form, with different Si/Al ratios, were provided by the French Institute of Petroleum. The MOR catalysts were prepared from the sodium form of mordenite with Si/Al = 6, supplied by Norton (Zeolon 900). The sample with Si/Al = 21 was obtained by acid leaching HMOR with  $\text{HNO}_3$  (4 M) at  $100^\circ\text{C}$ , and the sample with Si/Al = 108 was prepared by steaming the HMOR at  $650^\circ\text{C}$ , followed by acid leaching.

The introduction of copper into all the zeolites was performed by ion exchange with copper (II) acetate solution, following the method described elsewhere [22,23].

The Si/Al ratio was determined by XRF, IR spectroscopy and  $^{29}\text{Si}$  NMR and the copper content was analyzed by atomic absorption spectroscopy. The crystallinity of solids and the possible formation of copper oxides were investigated by powder X-ray diffraction. The copper exchange level was calculated by  $2 \times (\text{number of copper ions})/(\text{number of Al ions})$ . In the text, the catalysts will be labeled as, for example, CuMFI-11-40 (copper-zeolite structure-Si/Al ratio-copper exchange level).

Table 1 shows the composition of all the copper exchanged catalysts used in this work.

### 2.2. Temperature programmed reduction (TPR) analysis

TPR measurements were performed after pretreatment of the catalysts. About 80 mg of catalyst were pretreated under He flow (50 ml/min) at  $550^\circ\text{C}$  for 1 h and then cooled to room temperature. Reduction of the catalyst was carried out by passing a flow of 20 ml/min of  $\text{H}_2$  (3 vol%)/Ar and raising the catalyst temperature from room temperature to  $900^\circ\text{C}$  at  $10^\circ\text{C}/\text{min}$ . The change in hydrogen concentration was monitored continuously with a thermal conductivity detector. The water produced during the reduction was trapped in a 5 Å molecular sieve column.

### 2.3. NO temperature programmed desorption (NO TPD) analysis

TPD analyses were performed after catalysts pretreatment, as described for TPR experiments. NO

Table 1  
Main characteristics of the copper exchanged catalysts

Catalyst	Si/Al	Cu (wt%)	Cu/Al	Cu exchange level (%)
CuMFI-11-40	11	1.4	0.2	40
CuMFI-11-80	11	3.4	0.4	80
CuMFI-11-140	11	5.6	0.7	140
HMFI-27-0	27	–	–	–
CuMFI-27-40	27	0.8	0.2	40
CuMFI-27-80	27	1.4	0.4	80
CuMFI-27-160	27	2.7	0.8	160
CuMFI-27-320	27	5.5	1.6	320
CuMFI-100-280	100	1.4	1.4	280
CuMOR-6-20	6	1.0	0.1	20
CuMOR-6-60	6	3.4	0.3	60
CuMOR-6-100	6	6.1	0.5	100
CuMOR-21-60	21	1.1	0.3	60
CuMOR-21-100	21	2.0	0.5	100
CuMOR-21-180	21	3.9	0.9	180
CuMOR-108-180	108	0.8	0.9	180
CuY-7-40	7	1.4	0.2	40
CuY-20-100	20	1.8	0.5	100
CuY-56-220	56	1.5	1.1	220
CuY-85-320	85	1.4	1.6	320

adsorption was carried out at room temperature by passing a flow of 50 ml/min of NO(1 vol%)/He for 30 min. Afterwards, the NO in the gas phase was removed with He (50 ml/min), until no NO was detected in the effluent. TPD experiments were then carried out from room temperature to 500°C, at 10°C/min, under He flow. The composition of gas desorbed from catalysts was continuously monitored by using a quadrupole mass spectrometer (Balzers QMS421) calibrated on standard mixture and following the masses 28, 30, 32, 44 and 46.

#### 2.4. Catalytic tests

The catalytic tests were carried out at atmospheric pressure in a fixed-bed flow reactor, using 0.5 g of catalyst pretreated in situ at 550°C for 1 h under helium flow (15 l/h). The reaction mixture, comprising NO (880 ppm), C<sub>3</sub>H<sub>6</sub> (800 ppm), O<sub>2</sub> (4%) and He as balancing gas, was passed over the catalysts at a total flow rate of 15 l/h, in a temperature range between 200°C and 600°C. The reactants and products were analyzed by an on-line gas chromatograph with a 5 Å Molecular Sieve column used to separate oxygen, nitrogen and carbon monoxide and a Poraplot Q column for the sep-

aration of carbon dioxide and hydrocarbons. Further details of the apparatus are supplied elsewhere [22]. The catalytic activity was evaluated in terms of NO conversion into N<sub>2</sub> as  $2 \times [N_2]_{out}/[NO]_{in}$  after ca. 3 h on stream, since at this time the reaction practically reached the steady state. The hydrocarbon conversion into CO<sub>2</sub> was calculated as  $[CO_2]_{out}/(3 \times [C_3H_6]_{in})$ .

### 3. Results

From Table 1, it can be observed that the preparation of copper catalysts from different zeolite structures, with different Si/Al ratios and copper contents, led to catalysts having a large range of Cu/Al ratios (from 0.1 to 1.6).

#### 3.1. Temperature-programmed reduction (TPR)

TPR has been used to identify and quantify the copper species in copper exchanged zeolites and to characterize their reducibility. According to the literature [24,25], the reactions involved in the reduction process are the following:



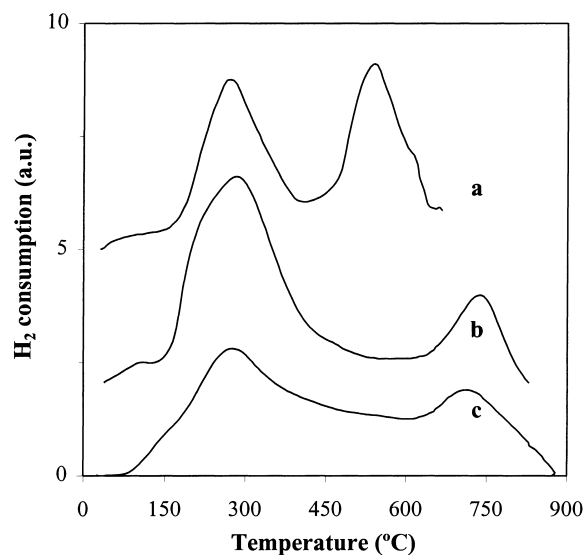
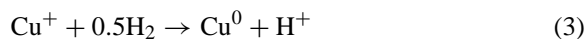


Fig. 1. Temperature-programmed reduction profiles of catalysts: (a) CuMFI-27-80; (b) CuMOR-21-60; and (c) CuY-20-100.



with both reactions (1) and (2) occurring within the same temperature range, lower than that for reaction (3).

Fig. 1 compares the TPR profiles obtained for three underexchanged catalysts CuMFI-27-80, CuMOR-21-60 and CuY-20-100 containing similar Si/Al ratios and copper contents. Table 2 presents the temperatures of the respective reduction processes.

Two reduction peaks were detected for all catalysts: the first at ca. 300°C and the second in the range 500–900°C. Comparing the area of the two peaks for each catalyst, and taking into account the previous considerations about the reduction temperature range of the different species of copper ( $\text{CuO}$ ,  $\text{Cu}^{2+}$ ,  $\text{Cu}^+$ ), it is possible to evaluate their presence in the studied samples.

CuMFI-27-80 catalyst shows two peaks with similar areas, the first being attributed to the reduction of  $\text{Cu}^{2+}$  to  $\text{Cu}^+$ , and the second to the reduction of the  $\text{Cu}^+$  formed during the previous reduction process. The similarity of the two peaks indicates the absence of other species besides  $\text{Cu}^{2+}$ . If the catalyst contained  $\text{CuO}$ , the first peak should be higher than the second,

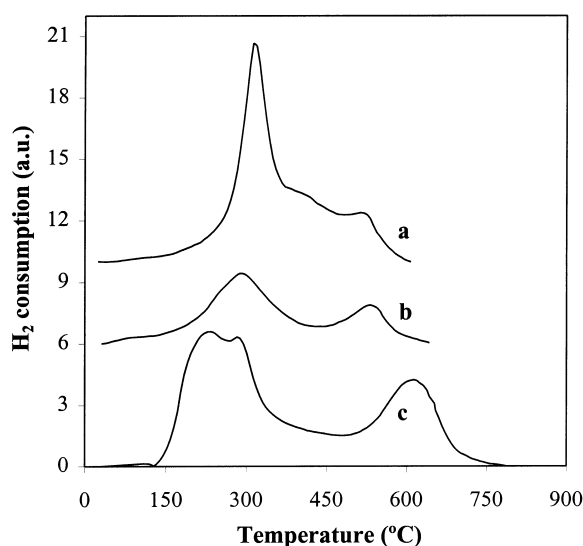


Fig. 2. Temperature-programmed reduction profiles of catalysts: (a) CuMFI-100-280; (b) CuMOR-108-180; and (c) CuY-85-320.

whereas if it contained  $\text{Cu}^+$  produced by the pretreatment (carried out by reducing atmosphere of He), the second peak should be the highest.

CuMOR-21-60 and CuY-20-100 catalysts do, however, present  $\text{CuO}$  species, in addition to isolated  $\text{Cu}^{2+}$ , because the first reduction peak has a greater area than the second one.

From Table 2, the analysis of the temperatures of the peak maxima shows the first peak occurring at similar temperatures for all the catalysts, while the second peak in CuMFI-27-80 appears at a lower temperature than for the two other catalysts. Considering that this second peak corresponds to the reduction of  $\text{Cu}^+$  ions to  $\text{Cu}^0$ , it means that the reduction of these ionic species is easier in the case of CuMFI catalysts. This is further supported by the final reduction temperature, which differs by about 200°C from CuMFI to CuY catalyst. The  $\text{H}_2$  TPR profiles of other series of CuMFI, CuMOR and CuY catalysts having high Si/Al ratios and overexchanged in copper, are presented in Fig. 2. The three profiles are significantly different, but all the catalysts present essentially two reduction peaks, the first one being more intense than the second, which means that copper oxide is present in these three catalysts besides isolated  $\text{Cu}^{2+}$  ions. For CuY-85-320 catalyst, the low-temperature peak presents two maxima, at 240 and 289°C, which can

Table 2

Temperatures related to the TPR profiles presented in Fig. 1

Catalyst	Temperature of peak maxima (°C)		Final reduction temperature (°C)
CuMFI-27-80	277	550	700
CuMOR-21-60	283	739	820
CuY-20-100	277	715	880

Table 3

Temperatures related to the TPR profiles presented in Fig. 2

Catalyst	Temperature of peak maxima (°C)			Final reduction temperature (°C)
CuMFI-100-280	319	403	520 <sup>a</sup>	600
CuMOR-108-180	289	532		640
CuY-85-320	240	289	620	780

<sup>a</sup> Shoulder.

be related to the two distinct reduction processes occurring at lower temperatures:  $\text{Cu}^{2+} \rightarrow \text{Cu}^+$  and  $\text{CuO} \rightarrow \text{Cu}^0$ . Regarding the temperatures reported on Table 3, the main differences are in the second peaks (related to the reduction of  $\text{Cu}^+$  ions to  $\text{Cu}^0$ ) and in the final reduction temperature. Once more, we verify that reduction of copper species is easier in the case of CuMFI catalyst, and the temperature to which all copper species are completely reduced follows the sequence  $\text{CuMFI} < \text{CuMOR} \ll \text{CuY}$ .

### 3.2. NO temperature-programmed desorption (TPD)

The NO TPD profiles obtained for the three catalysts, CuMFI-27-80, CuMOR-21-60 and CuY-20-100, containing similar Si/Al ratios and copper contents, are depicted in Fig. 3. All profiles are quite different. CuMFI-27-80 shows two NO desorption peaks, at ca. 120 and 390°C, the high-temperature peak being accompanied with oxygen desorption. In agreement with the literature [26,27], the low-temperature peak was ascribed to the desorption of NO from  $\text{Cu}^{2+}$ , while the second peak was associated with the decomposition of nitrate ( $\text{NO}_3^-$ ), nitrite ( $\text{NO}_2^-$ ) or  $\text{NO}_2^+$  adsorbed species [27]. CuMOR-21-60 catalyst presents only one NO desorption peak at ca. 100°C, while CuY-20-100 presents a peak at ca. 100°C and a 'shoulder' at ca. 160°C. The comparison of the three profiles also shows that the first peak is more intense for CuMFI-27-80 catalyst, followed by CuMOR-21-60 and, finally, by the CuY-20-100 catalyst that showed the smallest peak. Taking into account that this first

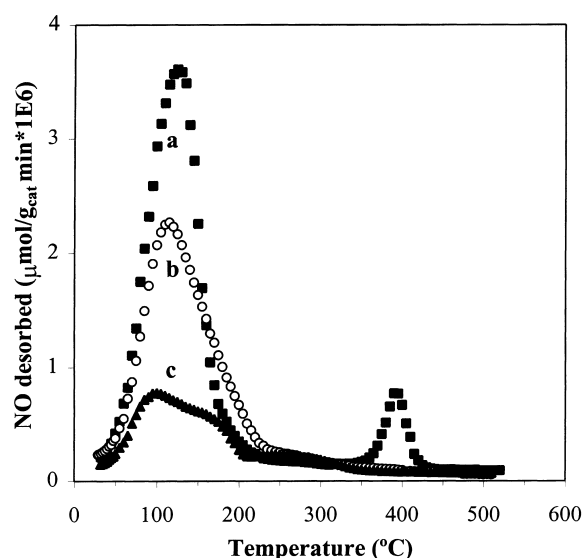


Fig. 3. NO temperature-programmed reduction profiles of catalysts: (a) CuMFI-27-80; (b) CuMOR-21-60; and (c) CuY-20-100.

peak is normally assigned to NO desorption from  $\text{Cu}^{2+}$ , we can conclude that CuMFI catalyst has a larger amount of this type of copper ions or, at least, they are more accessible to NO molecules than in the case of CuMOR and CuY catalysts.

Fig. 4 compares the NO TPD profiles obtained for the series of copper overexchanged catalysts (CuMFI-100-280, CuMOR-108-180 and CuY-85-320) with high Si/Al. The profiles corresponding to these three catalysts are also different. CuMFI-100-280 catalyst presents a first NO desorption peak with a maximum at ca. 120°C, and a

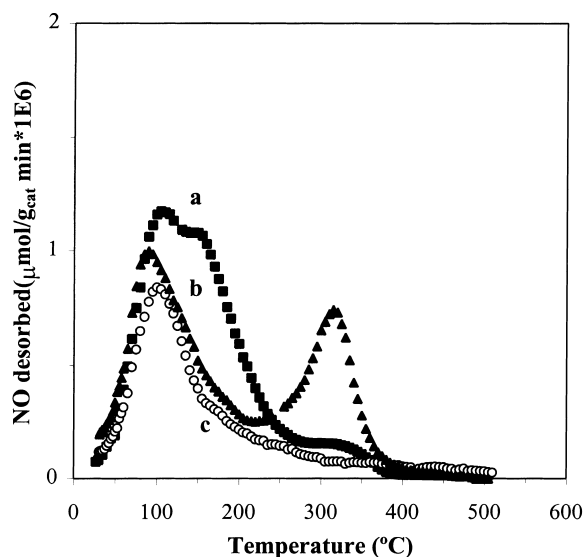


Fig. 4. NO temperature-programmed reduction profiles of catalysts: (a) CuMFI-100-280; (b) CuY-85-320; and (c) CuMOR-108-180.

‘shoulder’ at ca. 150°C. CuMOR-108-180 only shows a single peak with a maximum centered at ca. 100°C. On the other hand, CuY-85-320 catalyst presents two desorption peaks, the first one at 90°C and the second at 315°C, accompanied by oxygen desorption.

The previous results already showed that the NO adsorption capacity of the zeolites exchanged with copper depends on their structure. In order to better justify and support this observation, we present in Fig. 5 the amount of NO desorbed by three series of catalysts with different structure (CuMFI, CuMOR and CuY) as a function of Cu/Al ratio. In each one of the series, the catalysts differ in their Si/Al ratio but contain similar copper contents. CuMFI catalysts contain 1.4%, CuMOR contains ca. 1% and CuY ca. 1.5% of copper. The analysis of this figure shows that, for CuMFI and CuMOR catalysts, the total amount of desorbed NO decreases when the Cu/Al ratio increases, being higher for CuMFI catalysts in all the studied Cu/Al range. On the other hand, the amount of NO desorbed from CuY catalysts, is small and almost constant for  $\text{Cu/Al} \leq 1.1$ , slightly increasing for higher Cu/Al ratios.

As we have previously mentioned [23,28], the highest NO adsorption capacity in CuMFI and CuMOR catalysts with low Si/Al ratios is probably due to the highest concentration of Brønsted acid sites in these

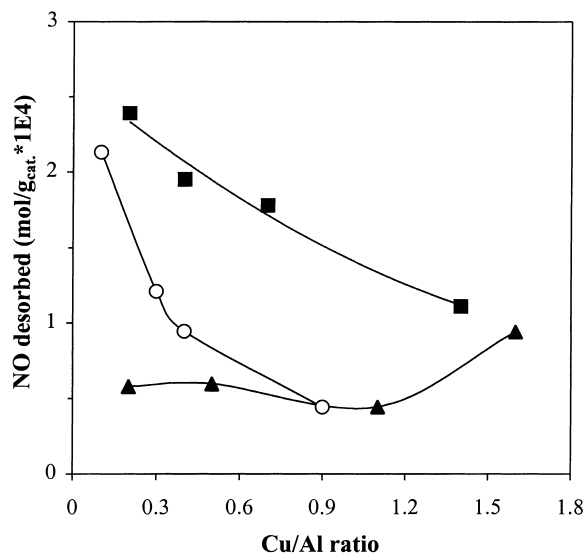


Fig. 5. Influence of the zeolite structure in the NO adsorption capacity of the catalysts: (■) CuMFI (with different Si/Al ratios and 1.4 wt% of copper); (○) CuMOR (with different Si/Al ratio and ca. 1 wt% of copper); and (▲) CuY (with different Si/Al and ca. 1.5 wt% of copper).

catalysts that can adsorb NO molecules. We had also suggested that the observed decrease of NO adsorption for overexchanged MFI catalysts is a consequence of the presence of large amounts of CuO species in these catalysts, which are less effective for NO desorption than  $\text{Cu}^{2+}$  ions. For CuMOR catalysts, the presence of CuO species in catalysts with Cu/Al ratio as low as 0.3 [23] justifies the strongest decrease of NO desorption capacity, in comparison with that of the MFI catalysts.

In the case of CuY zeolites, the low NO adsorption capacity observed for catalysts with  $\text{Cu/Al} \leq 1.1$ , is due to the location of Cu ions in hexagonal prisms and sodalite cavities of the faujasite structure, which are not accessible to NO molecules [29–32]. The increase in the amount of NO adsorbed by the catalyst with  $\text{Cu/Al} = 1.6$ , suggests that, although this catalyst (with  $\text{Si/Al} = 85$ ) contains about the same copper content as the other CuY zeolites, it has a greater copper concentration in the super cavities. Moreover, the low adsorption capacity of CuY catalysts is also due to CuO species that are present, in addition to  $\text{Cu}^{2+}$ , in all CuY samples, independently of their Si/Al ratio or copper content.

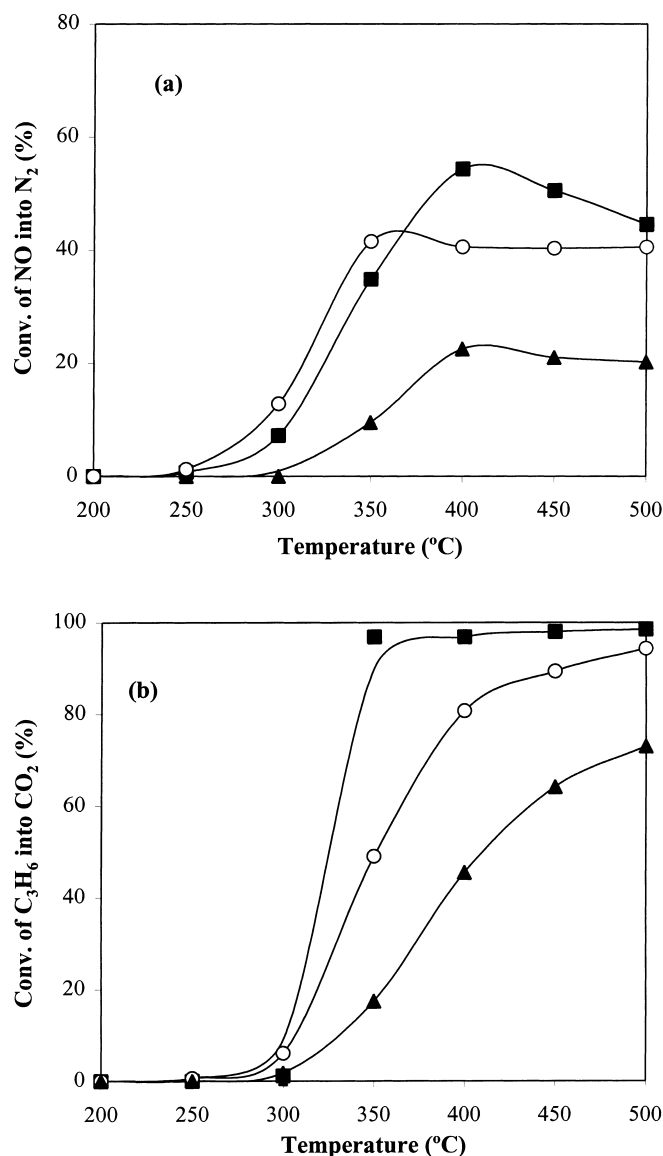


Fig. 6. Influence of zeolite structure on NO SCR with propene as a function of the temperature: (■) CuMFI-27-80; (○) CuMOR-21-60; and (▲) CuY-20-100.

### 3.3. Influence of the zeolite structure in the NO SCR activity with propene

In order to analyze the effect of the structure of the zeolite on NO reduction by propene, experiments were performed on several CuMFI, CuMOR and CuY catalysts with different Cu/Al ratios. Whenever possible, the comparisons of the results consider compa-

table Si/Al ratios, copper contents and type of copper species identified in the different catalysts.

The catalytic activities of CuMFI-27-80, CuMOR-21-60 and CuY-20-100 catalysts, that contain similar Si/Al ratios and copper contents, are compared on Fig. 6(a). The maximum NO conversion into N<sub>2</sub> and the most active temperature ( $T_{\max}$ ) clearly depend on the zeolite type. CuMFI-27-80 catalyst presents the

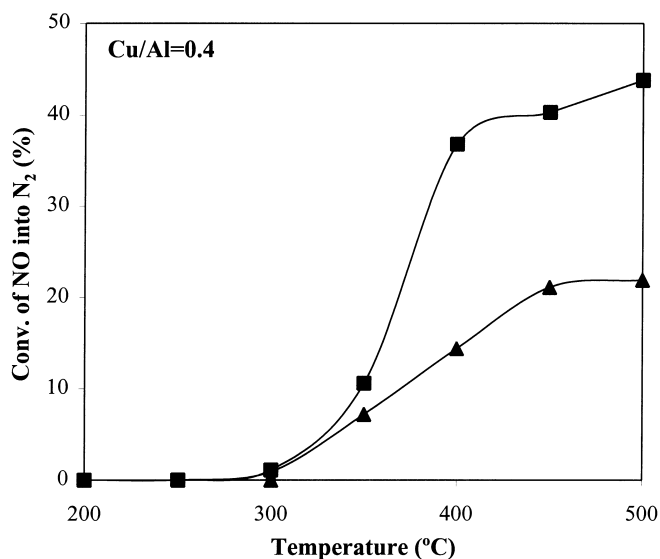


Fig. 7. Influence of zeolite structure on NO SCR with propene as a function of the temperature; both catalysts have Cu/Al=0.4: (■) CuMFI-11-40; and (▲) CuY-7-40.

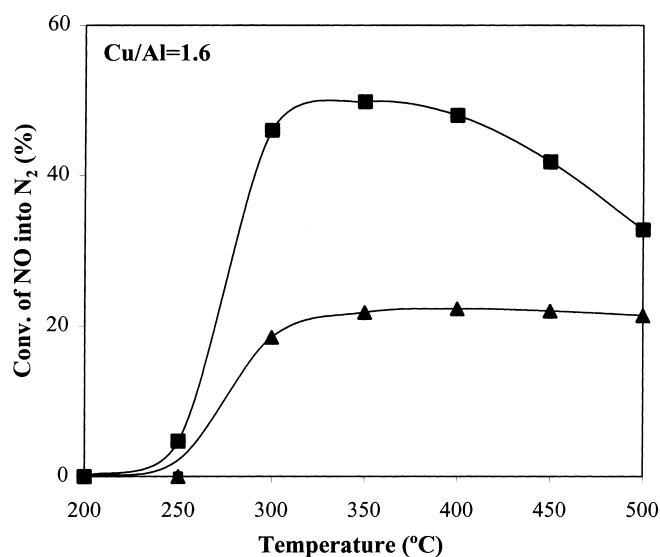


Fig. 8. Influence of zeolite structure on NO SCR with propene as a function of the temperature; both catalysts have Cu/Al=1.6: (■) CuMFI-27-320; and (▲) CuY-85-320.

highest maximum NO conversion into  $N_2$  (54%) at 400°C. CuMOR-21-60 presents an intermediate value (42%) relative to the maximum conversion observed for CuMFI and CuY, and nearly constant in the temperature range of 350–500°C. CuY-20-100 catalyst showed a very low maximum NO conversion (23%)

in the temperature range 400–500°C. Concerning the total propene oxidation in Fig. 6(b), one can see the same trends in all the temperature ranges.

Figs. 7–9 compare the catalytic activities of pairs of catalysts with different structures, identical Cu/Al ratio (or copper exchange level), but differing in their



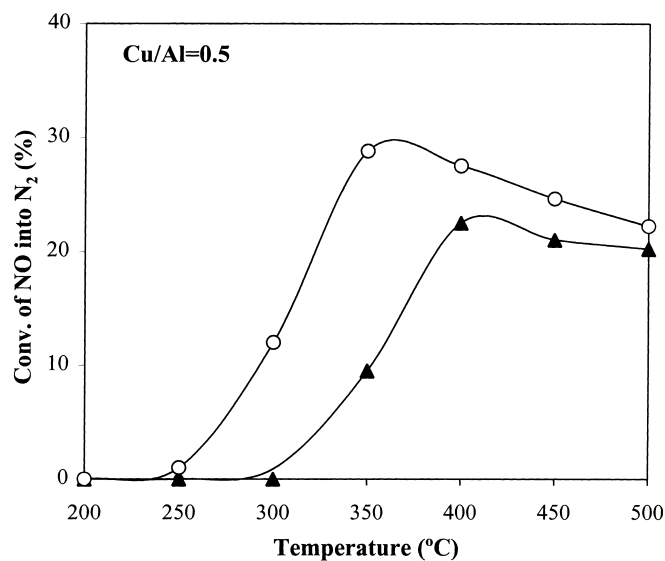


Fig. 9. Influence of zeolite structure on NO SCR with propene as a function of the temperature; both catalysts have Cu/Al=0.5: (○) CuMOR-6-100; and (▲) CuY-20-100.

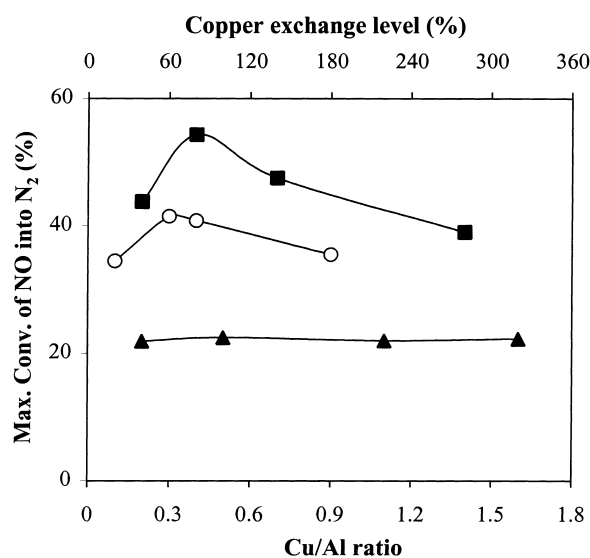


Fig. 10. Maximum nitrogen oxide conversion into nitrogen as a function of Cu/Al ratio: (■) CuMFI (with different Si/Al ratios and 1.4 wt% of copper); (○) CuMOR (with different Si/Al ratios and ca. 1wt% of copper); and (▲) CuY (with different Si/Al and ca. 1.5 wt% of copper).

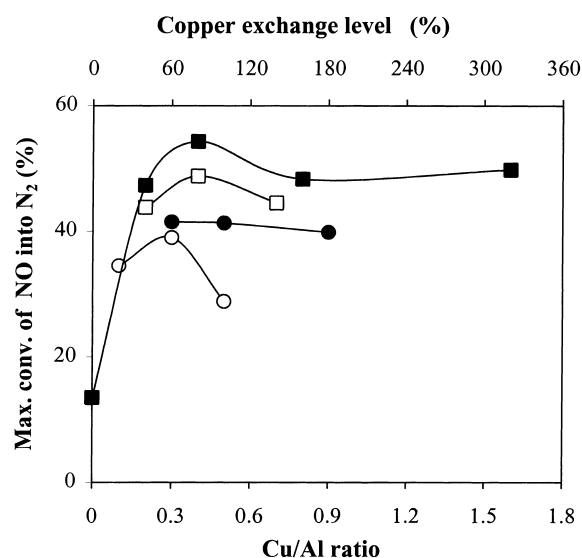


Fig. 11. Maximum nitrogen oxide conversion into nitrogen as a function of Cu/Al ratio: (□) CuMFI (with Si/Al=11 and different copper contents); (■) CuMFI (with Si/Al=27 and different copper contents); (○) CuMOR (with Si/Al=6 and different copper contents); and (●) CuMOR (with Si/Al=21 and different copper contents).

Si/Al ratios and copper contents. This set of figures clearly illustrates that the catalytic activity profiles for NO SCR with propene depend on the zeolite struc-

ture, either for underexchanged or overexchanged catalysts, CuY catalysts always being distinguished by their lowest activity.

Finally, in Figs. 10 and 11 we depict a more complete study that considers the evolution of maximum NO conversion into  $N_2$  obtained with several series of CuMFI, CuMOR and CuY catalysts, as a function of the Cu/Al ratio. Fig. 10 concerns three series of zeolites, each one having catalysts with different Si/Al ratios and similar copper contents. Fig. 11 presents the results of two sets of zeolite series (CuMFI and CuMOR) and, in this case, the catalysts that compose each one of the series have the same Si/Al ratio, but differ in their copper content. From the analysis of these figures, it can be noted that CuMFI catalysts are the most active, independently of Si/Al ratio and/or copper loading, followed by CuMOR and CuY catalysts.

#### 4. Discussion

The results shown in this work, in conjunction with those already presented and discussed in previous papers [22,23,28,33], show that the structure of the zeolite affects the nature and reducibility of copper ions, NO adsorption and also the catalytic behavior for NO SCR with propene.

For CuMFI catalysts, our results already published [22,28,34] showed that, in the case of underexchanged catalysts, copper is mainly present as  $Cu^{2+}$  ions while, in overexchanged catalysts, CuO species, isolated  $Cu^{2+}$  and  $Cu^+$  ions were detected. ESR and FTIR analysis confirmed those results and showed the presence of  $Cu^+$  ions mainly in overexchanged catalysts. For CuMOR we observed [23] that, in catalysts with copper exchange of  $\leq 20\%$ , the copper is in the form of isolated  $Cu^{2+}$  ions whereas, at higher copper exchange CuO species are also present.

In the case of CuY catalysts, we have shown here the  $H_2$ -TPR and NO TPD results for just two samples (Figs. 1–4), but we observed in all the studied CuY catalysts [35] the presence of isolated  $Cu^{2+}$  and CuO species independently of their Si/Al ratio or copper exchange level. Moreover, we observed that the complete reduction of the copper species present in CuY catalysts occurs at slightly lower temperatures for the overexchanged catalysts. From Fig. 10, it is quite evident that this type of catalysts present a low catalytic activity (maximum NO conversion observed for all CuY catalysts was about 20%) for SCR of NO

with propene, and which is independent of Cu/Al ratio. Campa et al. [30], having studied the influence of the copper loading in CuY catalysts, found that catalysts with  $<2\%$  copper content were not active for NO decomposition. They explained this result on the basis of the preferential location of  $Cu^{2+}$  ions after thermal treatments in SI sites (in the center of hexagonal prisms), which are not accessible to NO molecules. Dedeczek et al. [32] also proposed that, in Y zeolites, the copper ions that occupy the exchange sites SI, SI' and SII' are not accessible to NO molecules, only the copper ions located in the large cavities being accessible to NO.

In Fig. 10, we show that CuMFI catalysts are the most active, independently of the Cu/Al ratio. The maxima observed in the curves corresponding to MFI and MOR catalysts also indicate that there is a clear dependence between the catalytic activity of the studied catalysts and their composition, in terms of copper and Al contents (the highest value of maximum NO conversion into  $N_2$  was obtained for CuMFI catalysts with Cu/Al=0.4 and 80% of copper exchange level, and for CuMOR catalyst with Cu/Al=0.3 and 60% of copper exchange level). On the contrary, in the case of CuY catalysts no such dependence seems to exist.

A first approach to explain the differences in the catalytic activity observed between the three series of catalysts with different structures could come from considering the corresponding differences in NO adsorption capacity shown in Fig. 5, which suggests that the most active catalysts are those that have a higher tendency to adsorb NO. Li et al. [36] also suggested that the catalytic activity of a catalyst to NO conversion is proportional to its NO adsorption capacity at room temperature. These authors considered that the traditional intrinsic properties of the zeolites (e.g. acidity and shape selectivity), did not influence the reaction of NO reduction with hydrocarbons, the electronic effect originated by the zeolitic structure in the cations being more important.

The shape of each one of the curves corresponding to CuMFI and CuMOR, and the different location of the maximum of the curves, cannot however be explained only on the basis of the NO adsorption capacity. They have been previously explained [22,23,28,33], by taking into account the variation of acidity and the copper species ( $Cu^{2+}$ ,  $Cu^+$  and CuO) present in the catalysts as a function of the Cu/Al ratio.

In both series, the lowest NO conversions observed at lower Cu/Al ratios have been attributed to the higher acidity of the catalysts, which is not favorable to NO reduction by propene. The catalysts that present the highest maximum NO conversion into  $N_2$ , correspond to those that contain a higher concentration of  $Cu^{2+}$  (e.g. Cu-MFI-27-80 with Cu/Al = 0.4), and lower tendency to promote the agglomeration of the copper and formation of CuO species. In the case of CuMFI catalysts, the CuO species were only detected for overexchanged samples (Cu/Al > 0.5), which explains the observed decrease of the curve for higher Cu/Al ratios. In CuMOR catalysts, the CuO species already present in catalysts with Cu/Al  $\geq$  0.3 (e.g. CuMOR-21-60), are responsible for the shift of the maximum of the curve to lower Cu/Al ratios, and for the decrease in the maximum NO conversion observed at higher Cu/Al ratios.

In contrast to CuMFI and CuMOR catalysts, the CuY catalysts studied showed identical values of maximum NO conversion into  $N_2$ , independently of their Cu/Al ratios. The differences in activity found for these catalysts [35] only concern an extension for lower temperatures of the active-temperature window, for catalysts with higher Si/Al ratio. This behavior has been attributed to a decrease of the number of Brønsted acid sites, that are not favorable to SCR of NO with propene, as we have previously shown for CuMFI and CuMOR catalysts [22,33]. The results obtained by  $H_2$ -TPR, and TPD of NO in CuY catalysts, did not show appreciable differences in the type of copper species. It means that the distribution of copper species is comparable in all CuY catalysts, not depending on the zeolite composition (Cu/Al ratio). All the catalysts showed CuO species, and the number of isolated  $Cu^{2+}$  ions accessible to reactants should be practically constant. Regarding the role attributed to the different copper species in catalytic behavior of the other series of catalysts, the low activity exhibited by all CuY samples can be attributed, both to the presence of CuO species and to the reduced accessibility of reactants to copper ions.

Taking into account all the results reported up to now for the three types of zeolites, we verified that, in all the cases, it was possible to explain the differences in the catalytic activity based on the copper species detected for each sample. We have proved that the zeolite structure affects the nature of the copper that is incorporated in catalysts with similar chemical com-

positions. We have put forward evidence that the different copper species present in the zeolites are not equally active for NO reduction with propene, and that the activities of catalysts can be correlated with accessibility and concentration of  $Cu^{2+}$  ions and with copper dispersion (or presence of agglomerates of CuO).

The identification of the copper species was carried out on as-prepared samples, but we extracted from used catalysts (CuMOR and CuMFI) similar conclusions [37,38] confirming the importance of the isolated  $Cu^{2+}$  species for NO SCR with propene. It is also important to note that the characterization of copper species was performed after pretreatment of the samples under conditions which were far from the lean  $NO_x$  operating regime which is normally strongly oxidizing and favors the stabilization of  $Cu^{2+}$ . Although the methods used do not offer information on the reaction conditions, the extrapolation of the characterization results to reaction led to coherent conclusions for all the studied Cu-catalysts.

Following the statements outlined above, it appears possible to draw from our results some inferences that reinforce the opinion of the authors who consider:

1. NO SCR reaction mechanism proceeds via a pathway that includes  $Cu^{2+}$  ions (formation of  $Cu^{2+}$ - $NO_2$  complexes [14]);
2. the promoting role of oxygen is associated with its ability to oxidize NO to  $NO_2$ , and stabilize the system by preventing reduction of  $Cu^{2+}$  to lower valence states [7,8];
3. a high dispersion of the Cu is desirable [14,39]; and
4. CuO species are inactive and/or restrict the access to the isolated  $Cu^{2+}$  ions [26,40].

In summarizing, we think that the main effect of the zeolite structure is to create conditions to lodge the metal in a peculiar environment that provides the dispersion and stabilization of isolated copper ions and avoids the formation of clusters of CuO species.

## 5. Conclusions

This work has shown that the zeolite structure affects copper nature, its reducibility, NO adsorption capacity and the catalytic performances for SCR of NO with propene. CuMFI catalysts are the most active,

independently of Si/Al ratio and copper content, followed by CuMOR and CuY catalysts. CuMFI catalyst that presents the highest concentration of isolated  $\text{Cu}^{2+}$  is the most active catalyst, confirming the importance of these species in NO SCR, as shown in previous works. CuO species existing in CuMOR, and mainly in CuY, are responsible for the lower activity of these catalysts, when compared with that observed on CuMFI at similar Cu/Al ratios.

The results show that catalytic improvements are possible, and point to the importance of finding materials whose structural features favor the formation of isolated  $\text{Cu}^{2+}$  species.

## References

- [1] M. Iwamoto, H. Yahiro, *Catal. Today* 22 (1994) 5.
- [2] M. Shelef, *Chem. Rev.* 95 (1995) 209.
- [3] K.C.C. Kharas, D.-J. Liu, H.J. Robota, *Catal. Today* 26 (1995) 129.
- [4] A.P. Walker, *Catal. Today* 26 (1995) 107.
- [5] W.K. Hall, J. Valyon, *Catal. Lett.* 15 (1992) 311.
- [6] V.I. Părvulescu, P. Grange, B. Delmon, *Catal. Today* 46 (1998) 233.
- [7] J.O. Petunchi, W.K. Hall, *Appl. Catal. B* 2 (1993) L17.
- [8] J.O. Petunchi, W.K. Hall, *Appl. Catal. B* 3 (1994) 239.
- [9] M. Shelef, C.N. Montreuil, H. W. Jen, *Catal. Lett.* 26 (1994) 277.
- [10] P. Ansell, A.F. Diwell, S.E. Golunski, J.W. Hayes, R.R. Rajaram, T.J. Truex, A.P. Walker, *Appl. Catal. B* 2 (1993) 81.
- [11] R. Burch, P.J. Millington, *Appl. Catal. B* 2 (1993) 101.
- [12] T. Inui, S. Iwamoto, S. Kojima, S. Shimizu, T. Hirabayashi, *Catal. Today* 22 (1994) 41.
- [13] D.J. Lui, H.J. Robota, *Appl. Catal. B* 4 (1994) 155.
- [14] B.J. Adelman, T. Beutel, G.-D. Lei, W.M.H. Sachtler, *J. Catal.* 158 (1996) 327.
- [15] C. Yokoyama, M. Misono, *Catal. Today* 22 (1994) 59.
- [16] Y. Li, J.N. Armor, *J. Catal.* 150 (1994) 376.
- [17] S. Sato, Y. Yu-u, H. Yahiro, N. Mizuno, M. Iwamoto, *Appl. Catal.* 70 (1991) L1.
- [18] M. Iwamoto, H. Yahiro, N. Mizuno, in R. von Ballmoos et al. (Eds.), *Proceedings 9th International Zeolite Conference*, Montreal, 1993, 397 pp.
- [19] B. Wichterlová, J. Dedeczek, Z. Sobalík, A. Vondrová, K. Klier, *J. Catal.* 169 (1997) 194.
- [20] B. Wichterlová, Z. Sobalík, A. Vondrová, *Catal. Today* 29 (1996) 149.
- [21] D.J. Parrillo, J.P. Fortney, R.J. Gorte, *J. Catal.* 153 (1995) 190.
- [22] C. Torre-Abreu, M.F. Ribeiro, C. Henriques, F.R. Ribeiro, *Appl. Catal. B* 11 (1997) 383.
- [23] C. Torre-Abreu, M.F. Ribeiro, C. Henriques, G. Delahay, *Appl. Catal. B* 14 (1997) 261.
- [24] J. Sárkány, J.L. d'Itri, W.M.H. Sachtler, *Catal. Lett.* 16 (1992) 241.
- [25] S.J. Gentry, N.W. Hurst, A. Jones, *J. Chem. Soc. Faraday Trans. I* 75 (1979) 1688.
- [26] B. Coq, D. Tachon, F. Figueras, G. Mabilion, M. Prigent, *Appl. Catal. B* 6 (1995) 271.
- [27] W. Zhang, H. Yahiro, N. Mizuno, J. Izumi, M. Iwamoto, *Langmuir* 9 (1993) 2337.
- [28] C. Torre-Abreu, M.F. Ribeiro, C. Henriques, G. Delahay, *Appl. Catal. B* 12 (1997) 249.
- [29] M. Iwamoto, S. Yokoo, K. Sakai, S. Kagawa, *J. Chem. Soc. Faraday Trans. I* 77 (1981) 1629.
- [30] M.C. Campa, V. Indovina, G. Minelli, G. Moretti, I. Pettiti, P. Porta, A. Riccio, *Catal. Lett.* 23 (1994) 141.
- [31] J. Valyon, W.K. Hall, *J. Phys. Chem.* 97 (1993) 1204.
- [32] J. Dedeczek, Z. Sobalik, Z. Tvaruzková, D. Kaucky, B. Wichterlová, *J. Phys. Chem.* 99 (1995) 16327.
- [33] C. Torre-Abreu, M.F. Ribeiro, C. Henriques, F.R. Ribeiro, *Appl. Catal. B* 13 (1997) 251.
- [34] C. Henriques, M.F. Ribeiro, C. Abreu, D.M. Murphy, F. Poignant, J. Saussey, J.C. Lavalley, *Appl. Catal. B* 16 (1998) 79.
- [35] C. Torre-Abreu, PhD Thesis, IST, 1996.
- [36] Y. Li, J.N. Armor, *Appl. Catal. B* 2 (1993) 239.
- [37] C. Torre-Abreu, M.F. Ribeiro, C. Henriques, F.R. Ribeiro, *Catal. Lett.* 43 (1997) 25.
- [38] C. Torre-Abreu, M.F. Ribeiro, C. Henriques, F.R. Ribeiro, *Catal. Lett.* 43 (1997) 31.
- [39] W. Grünert, N.W. Hayes, R.W. Joyner, E.S. Shiro, M.R.H. Siddiqui, G.N. Baeva, *J. Phys. Chem.* 98 (1994) 10832.
- [40] C. Lee, K. Choi, B. Ha, *Appl. Catal. B* 5 (1994) 7.